The Effect of *N,N*-Dimethylformamide and Polymer Grafting on the Morphology of Polyester Fibers in Fabric Substrate

HOWARD L. NEEDLES* and MYUNG-JA PARK†

Division of Textiles and Clothing, University of California, Davis, California 95616

SYNOPSIS

Photo-induced graft polymerization of acrylic acid (AA) and methyl acrylate (MA) in the liquid and vapor phase, respectively, onto *N,N*-dimethyformamide (DMF)-pretreated poly(ethylene terephthalate) (PET) fibers in fabric substrate was studied. The effect of various synthesis conditions and DMF pretreatment on the graft yields on PET was investigated. The internal morphology and properties of DMF-pretreated and grafted PET fibers in the fabric were characterized using density and birefringence measurements, differential thermal analysis (DTA), Fourier transform infrared spectroscopy (FTIR), dyeing methods, and critical dissolution times. The grafting was promoted by increasing DMF pretreatment temperature and the amount of DMF retention in the PET. Increasing biacetyl and monomer flow time and irradiation time enhanced grafting. DMF pretreatment resulted in increases in total void content, degree of crystallinity, *trans*-isomer content, chain folding, segmental mobility, and molecular packing of the PET, but caused decreases in its amorphous orientation, intermolecular forces, and individual void size through longitudinal shrinkage, lateral swelling, and removal of oligomers.Subsequent graft copolymerization led to further changes in the internal morphology and properties of the PET. PET grafted with AA had a higher cohesive energy density, lower degree of molecular packing, and larger individual void size, but less total void content, lower segmental mobility, less chain orientation, and a lower degree of crystallinity. PET grafted with MA showed increases in total void content, individual void size, segmental mobility, and molecular packing, but showed decreases in chain orientation and degree of crystallinity. © 1996 John Wiley & Sons, Inc.

INTRODUCTION

Poly(ethylene terephthalate) (PET) is a very important fiber due to its desirable physical and chemical properties, but its chemical inertness, hydrophobicity, and high crystallinity cause problems in the areas of dyeing, comfort, and static buildup. Photo-induced graft polymerization[1–10] is one of the most effective methods to modify the PET chemically and physically. Using various monomers the fiber properties of linear homopolymer PET can be controlled and modified through the formation of branched copolymer. However, there is a problem in obtaining deep uniform grafting of monomers onto PET fibers due to their high crystallinity. Swelling of PET by solvent treatment prior to graft copolymerization[3,8,11] has been shown to be effective for deeper uniform grafting into PET fibers.

This physical modification of PET by solvent pretreatment and photo-induced chemical modification by graft polymerization results in the changes in the molecular structure and intermolecular organization of the fiber.[4,6–10,12] These are defined in this work as the internal morphology including chain orientation, molecular conformation, intermolecular forces, degree of crystallinity, molecular packing, void structure, and segmental mobility. The internal morphology of DMF-treated PET has been studied extensively[13–20] and is well known, whereas the effect of photo-initiated graft copolymers on the internal

* To whom all correspondence should be addressed at his current address: 987 Customs Road, Pebble Beach, CA 93953.

† From the Ph.D. dissertation of M.-J. Park, University of California, Davis, 1992.

Journal of Applied Polymer Science, Vol. 59, 1683–1698 (1996)
 CCC 0021-8995/96/111683-16

morphology of DMF-treated PET has not been studied thoroughly.[8]

In this study, the specific aims are twofold: first, to obtain graft copolymers of PET by photo-induced graft polymerization of acrylic monomers onto PET fabric using the vapor phase or liquid phase methods, establish the effect of grafting conditions on graft yield, and determine the effect of the DMF pretreatment on the grafting process. The second is to characterize the internal morphology of the grafted PET using various techniques and to examine selected fiber properties comparing these changes with those of DMF-pretreated PET.

EXPERIMENTAL

Materials

Dacron Type 54 polyester (PET) fabric, style #767 from Testfabrics, Inc., was used. Acrylic acid (AA), methyl acrylate (MA), and biacetyl were reagent grade chemicals from Aldrich Chemical Co. *N,N,*-Dimethylformamide (DMF) and phenol were reagent grade from Fisher. DMF was used after distillation (BP = 153°C). A commercial poly(acrylic acid) (PAA) sample from Aldrich, in powder form with a molecular weight of 250,000 and a T_g of 106°C, was used for comparison with PET-*g*-PAA.

Four disperse dyes were chosen due to their structural differences in size and shape: p-Nitroaniline (M_w = 138.13, 225 cubic Å), C.I. Solvent Yellow 7 (p-phenyl azophenol, M_w = 198.23, 335 cubic Å), C.I. Disperse Red 15 (1-amino-4-hydroxyanthraquinone, M_w = 238.23, 450 cubic Å), and C.I. Solvent Green 3 [1,4-(4-methylphenyl amino) anthraquinone, M_w = 418.50, 4200 cubic Å). Dye size was approximated as the volume in cubic Angstroms of the smallest box that would contain a particular dye molecule.[15] All dyes were greater than 95% pure, obtained from Aldrich Chemical Co., and purified by recrystallization from suitable solvents.

DMF Pretreatment Procedure

The polyester fabric samples (10 × 20 cm^2) were immersed in DMF at 100, 120, and 140°C for 10 min without tension. After treatment, DMF-treated fabrics were air dried or oven dried in the vacuum oven at 60°C for 48 h. The weight loss of DMF-treated samples was determined by weighing the conditioned specimens before and after DMF treatment. The washed samples after DMF treatment were conditioned at 21°C and 65% relative humidity for 24 h before weighing. Longitudinal shrinkage of DMF-treated samples was calculated by length differences before and after DMF treatment at room temperature.

Characterization Techniques

Ten yarn specimens (about 15 cm) were prepared by unraveling the warp yarn from the DMF-treated fabrics and grafted fabrics. One end of each specimen was fastened vertically by a clip, and the other end of the yarn was supported by a 50 g weight to remove the crimp from the specimen. The 10 cm length of each yarn was obtained by cutting it on the mark first, then at the edge of the clip. The measured 10 yarns were weighed, and represented in g/1000 m (tex). Four replications were made and the results were averaged.

Fiber diameters of DMF-treated PET and grafted PET samples were measured through use of a calibrated optical microscope. Fifty replicas were made and the results were averaged.

Vapor Phase Photografting

Photo-initiated vapor-phase grafting of methyl acrylate onto PET fibers in the presence of biacetyl was carried out at room temperature and under a nitrogen atmosphere, using a photoreactor system described previously.[7]

Prior to graft polymerization, two polyester fabric samples (10 × 20 cm^2) pretreated with DMF were stapled onto a cylinder-shaped screen. The screen with attached samples was placed in a 3-liter resin reaction kettle so that it conformed to the wall. In the center of the reactor was a Pyrex cold finger containing a UV lamp. A high-pressure quartz mercury-vapor lamp (Ace-Hanovia Lamp Cat. No. 6515–32, from Ace Glass Inc.) was used as a source of ultraviolet (UV) radiation. The lamp wattage was 200 W and the arc-length was 12 cm. The distance between the lamp and the fabric surface was 6 cm.

Biacetyl was used as a photosensitizer to initiate the reaction effectively. It is placed in a gas bubbler, and biacetyl vapors carried by nitrogen gas (10 cc/s) were allowed to flow into the reactor through the gas inlet located in the top of the reactor. Biacetyl vapor diffused onto the sample fabric, and initial flushing of biacetyl and nitrogen expelled the oxygen and moisture in the system through the gas outlet and prevented inhibition of the photo reactions. After initial flushing of biacetyl for a given length of time, its flow was continued during irradiation and monomer flow.

Methyl acrylate monomer was placed in the bubbler through which nitrogen was bubbled, and monomer vapor was carried into the reactor at 10 cc/s for a given length of time with simultaneous or subsequent irradiation.

Photografting was terminated by ceasing the irradiation and monomer and biacetyl flow. Then samples were removed from the reactor and washed in boiling water for 3 h, air dried, conditioned, and weighed. Reaction conditions for the PMA photografting procedures, MA monomer uptake, and selected properties of the graft copolymers (PET-*g*-PMA) were examined.

Liquid Phase Photografting

Photo-initiated liquid-phase grafting of acrylic acid onto PET fibers was carried out under the same experimental conditions as vapor-phase photografting mentioned previously except for introduction of the monomer. The DMF-pretreated polyester fabrics were presoaked with various amounts of AA monomer, and excess monomer was removed to a wet pickup of usually 50%. Then, two sample fabrics were placed in the reactor and irradiated in the presence of biacetyl. After termination of photografting, PAA homopolymers were removed by washing with boiling water for 3 h. The sample fabrics were air dried, conditioned, and weighed. Reaction conditions for the PAA photografting procedures, AA monomer uptake, and selected properties of graft copolymers (PET-*g*-PAA) were examined.

Graft Yield Calculations

The degree of grafting was determined by weight gain according to the following equation:

$$\text{graft yield (\%)} = \frac{W_1 - W_0}{W_0} \times 100$$

where W_0 is the conditioned sample weight before grafting, and W_1 is the conditioned sample weight after grafting and washing the homopolymer. In the case of PET-*g*-PAA copolymer, graft yield was corrected for water held by the PAA graft.

Characterization

Densities for DMF-treated PET, PET-*g*-PAA, and PET-*g*-MA were determined by floatation in a density gradient column of heptane and carbon tetrachloride at 21°C.

The crystallinity of untreated PET and DMF-modified PET fibers (X_{PET}) was calculated from the density measurement of the fibers (d) by the following equation:

$$\frac{1}{d} = \frac{X_{PET}}{d_c} + \frac{1 - X_{PET}}{d_a}$$

The crystalline density (d_c) and the amorphous density (d_a) of PET determined by previous studies in our laboratory were 1.457 g/cm^3 and 1.336 g/cm^3, respectively. The crystallinity of graft copolymers (X_{CO}) was calculated from the crystallinity of PET and the increased amorphous content by grafting (G) by the following equation:

$$X_{CO} = \frac{X_{PET}}{1 + G}$$

Each sample (5 × 5 cm^2) of the untreated, DMF-modified, and grafted PET fabrics was dyed in an aqueous infinite dye bath at 100°C for 1/2 h and 6 h without using dispersing agents and carriers. The liquor ratio was 100:1 (owf). The dyed fabrics were washed with hot water. The dyes were extracted from each dyed sample using 10% phenol in DMF, and the dye concentrations were measured photometrically with a Hitachi U2000 Spectrophotometer. Dye concentrations were calculated from absorbance with interpolation of their concentration from calibration curves. Dye concentrations were expressed in μmol/1 g of dry fabric.

Solvent diffusion properties of the sample fibers were determined by measuring their critical dissolution times (CDT) in phenol. CDT was measured by suspending 5 cm loops of warp yarns unravelled from the sample fabrics. The specimens were supported with a stainless hook at the top end and a 1 g copper weight at the bottom end of them in the container filled with pure phenol at 60 and 80°C. The time measurement started when the hooked specimen was put into phenol and ended when a copper weight reached the bottom of the container with the specimen breaking. An average of 10 replicates was taken.

The variations in stereochemistry and spatial arrangement of the sample fibers were investigated with the vibrational spectrum of PET in the range of 4500 to 500 cm^{-1}, especially the 1100 to 600 cm^{-1} region, using a FTIR (Perkin–Elmer model 1600 series). For quantitative analysis of molecular orientation, the amounts of trans and gauche conformation were determined by the relative intensity of

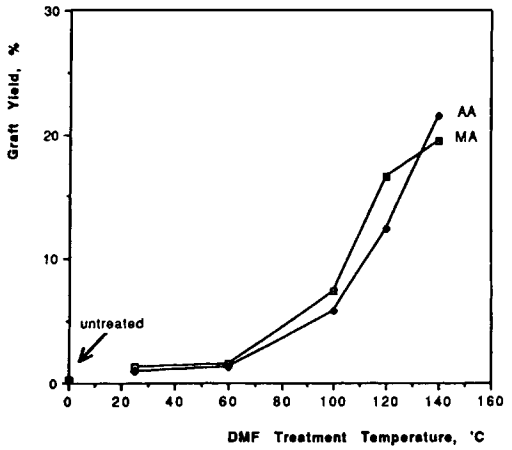

Figure 1 Effect of DMF treatment temperature on photografting of MA and AA onto DMF-pretreated PET.

the 973 and 875 cm^{-1} infrared absorption band, respectively. The intensity of the 973 and 875 cm^{-1} bands (C—O stretching mode of the ethylenedioxy linkage in the *trans* and gauche conformation, respectively) relative to the intensity of the 795 cm^{-1} band (a normal mode of the p-benzenoid linkage, used to correct for thickness variations) were measured. The fold conformation of polymer chains at the surface of folded chain was detected by the 988 cm^{-1} absorption band.[21,22]

The degree of crystallinity was calculated with the relative intensity of trans conformation according to the following equation:[13]

$$X = 12.13 - \frac{265.00}{\frac{A_{973}cm^{-1}}{A_{795}cm^{-1}} + 21.26}$$

where X is crystallinity, A_{973} cm^{-1} and A_{795} cm^{-1} are absorbance at wavelength 973 and 795 cm^{-1}, respectively.

The chain orientation along the fiber axis in the molecular structure of the sample fibers was determined by refractive indices and birefringence through anisotropy. The refractive indices (n) of sample fibers were measured by the liquid immersion method with an optical microscope with polarized light at room temperature using standard refractive index liquids from Cargille.

Differential thermal analysis of approximately 3 mg (or 10 mg for T_g measurement) of samples finely chopped by scissors were measured using a Mettler TA 2000M Thermal Analysis System under a nitrogen atmosphere at a heating rate of 5°C/min. Al_2O_3 was used as a reference. Glass transition temperatures (T_gs) were determined from these analyses.

A table model Instron Universal Testing Machine was used to measure tensile properties of samples. Gauge length (7.6 cm) of warp yarns were measured at 20 cm/min constant rate of elongation at 65% relative humidity and 21°C. At least 25 tests were averaged for each sample.

Scanning Electron Micrographs (SEM) of samples were obtained through use of an International Scientific Instrument model DS130 Microscope. Before scanning, fiber samples were sputter coated with gold.

RESULTS AND DISCUSSION

Effect of DMF-Pretreatment on Grafting

The effect of DMF pretreatment temperature and DMF retention in DMF-treated PET on photografting of AA and MA were investigated. The results are represented in Figures 1 and 2, respectively. As shown in Figure 1, the DMF pretreatment provides dramatic increases in graft yields with increasing DMF treatment temperature. Without DMF pretreatment, little grafting of AA and MA occurred. Figure 2 shows that the residual DMF in DMF-treated PET affects the grafting of AA and MA remarkably. The oven-dried PET sample, where there is no DMF residue, shows much lower graft yields than air-dried PET that has never been dried completely.

The level of graft yield correlated well with changes in fiber diameter, longitudinal shrinkage, weight loss of the fiber after DMF treatment (which is shown in Fig. 3), and some parameters of internal morphology and selective properties of DMF-treated PET fibers. Lateral swelling of the fiber, removal of

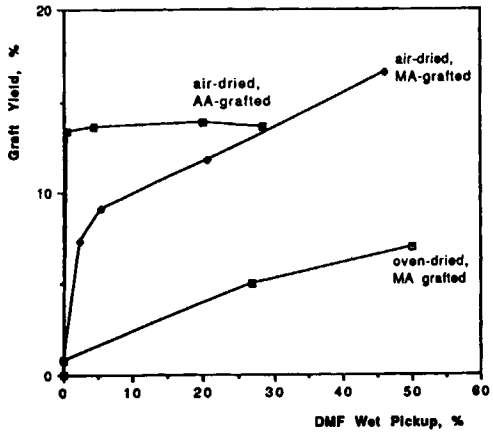

Figure 2 Effect of DMF retention in DMF-pretreated PET on photografting of MA and AA.

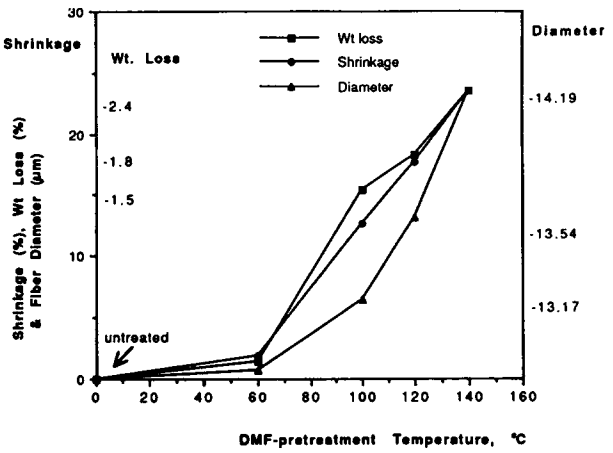

Figure 3 Effect of DMF pretreatment temperature on changes in fiber properties of PET.

low molecular weight oligomers, and DMF-induced recrystallization and rearrangement within PET fibers results in void formation that enhances its sorption and diffusion properties; the fast and deep diffusion of monomers into the fiber promotes high monomer uptake and the spreading out the grafting zone over the cross-section. Details of the changes in internal morphology of DMF-treated PET will be discussed later.

DMF retained in the DMF-treated PET has a very important role in grafting. DMF removal from the fiber by oven drying may cause complete or partial collapse of the DMF-swollen structure, whereas the remaining DMF in samples air dried at room temperature and exchanged with the monomers would lead to minimal collapse and support of the swollen structure to give the reaction for growing grafted chains. Weigmann et al.[19,23] have suggested that after removal of DMF, the small crystallites formed during DMF treatment cannot support the swollen structure and collapse; consequently, this results in the partial restoration of the original state. Also, residual DMF in the fiber may act as a plasticizer by interrupting the secondary forces between adjacent PET molecules and interacting with the ester groups in PET, allowing monomers to diffuse faster into the fiber to enhance grafting.

General Features of DMF-Treated PET

Both of the chemical action from the DMF and thermal energy take part in changing the fiber features. As shown in Figure 3, great changes in macro structure of the fiber occur after DMF treatment, such as axial shrinkage, increased diameter, and weight loss of the fiber. This alters fiber features and implies significant changes in its micro structure.

Surface morphology was examined by taking scanning electron micrographs of the untreated PET and DMF-modified PET fiber. Untreated PET showed a great number of tiny particles on the surface of untreated PET fiber assumed to be oligomers. Less of these particles were found on DMF-treated PET. Surface cavitation is not found in the oriented fibers used in this study.

The molecular orientation and conformation of DMF-modified PET was determined through FTIR spectroscopy. The FTIR scans for the untreated PET and DMF-treated PET fibers. The content of chain folding and *trans* and gauche isomers were calculated from these scans and listed in Table I.

The *trans* conformation is greater than gauche conformation for all fibers and it increases with increasing DMF treatment temperature. The crystals become larger and more perfect by chain rearrangement[24] to stabilize the shortened fiber, which causes an increase in the *trans* isomer formation. Usually the *trans* content has been determined for the drawn PET fibers. The stretched PET fibers have been shown to have an excellent correlation between total *trans* content and overall molecular orientation;[25,26] however, in the case of spun fibers, used in this study, correlation of amorphous

Table I FTIR Analysis of Relative Intensity and Concentration of Trans, Gauche, and Chain Fold in DMF-Treated PET Fibers

Treatment	Trans	Gauche	Chain Fold	% Trans	% Gauche
Untreated	1.261	0.391	[a]	76.3	23.7
DMF-treated at					
100°C	1.605	0.326	[b]	83.1	16.9
120°C	1.571	0.310	[b]	83.5	16.5
140°C	1.865	0.324	[b]	85.2	14.8

[a] Not apparent.
[b] Observable but not calculable.

Table II Crystallinity and Density of DMF-Treated PET Fibers

Treatment	Crystallinity by Density (%)	Crystallinity by FTIR (%)	Density (g/cc)
Untreated	42.6	36.3	1.3836
DMF-treated at			
100°C	48.1	54.0	1.3902
120°C	50.1	52.0	1.3924
140°C	51.7	67.0	1.3945

orientation to the overall orientation is seen.[26] In contrast to the above results, DMF-treated PET fibers showed an inverse relationship between *trans* content and amorphous orientation, as discussed later.

The spectra of the untreated PET has no or little indication of the 988 cm^{-1} absorption band, and the spectra of DMF-modified samples treated at 100 and 120°C have a little, whereas that of DMF-modified samples treated at 140°C shows a distinct 988 cm^{-1} absorption band. The higher the DMF treatment temperature, the greater the extent of chain folds in fibrils in crystalline areas that are formed. The extended state in the drawn polymer is favored to revert to the folded form in DMF, when the temperature is raised by thermal and kinetic energies. Chain folding occurs to make the stable form of the polymer chains during recrystallization in the contracted fiber. It must be one of the reasons of fiber shrinkage after DMF treatment and, consequently, lowers the amorphous orientation. The chain-folding content is well correlated with the *trans* isomer content.

The degree of crystallinity of DMF-treated PET fibers was calculated based on the content of *trans* isomers from the FTIR analysis and density measurements, respectively. The results are listed in Table II. The crystallinity increases with increasing DMF treatment temperature. With the increasing *trans* content, the degree of crystallinity tends to increase with the highest *trans* content and degree of crystallinity found in PET treated at 140°C. Also increased chain-folded crystals certainly cause an increase in crystallinity, as given in Table I. Other researchers have reported similar results.[17,19] Recrystallization and chain rearrangement occur to stabilize the swollen structure.

Chain compactness is considered from the results of the density, and the refractive indices (RI) of the fibers. DMF treatment leads to an increase in density and density values and increase with increasing DMF treatment temperature, which is shown in Table II. The perpendicular RIs ($n_\perp$) of the PET are only slightly affected by DMF treatment temperature, which is given in Table III.

The greater density values indicate the higher molecular packing in the DMF-modified PET fibers. DMF-induced recrystallization and chain rearrangement results in the chain compactness in the crystalline region, however, it is not correlated with the chain compactness in the amorphous regions where more voids are created and chains become more disordered, which will be discussed later. While the somewhat higher value in perpendicular RIs of PET fibers suggests a very slight decrease in molecular packing, it is not correlated with crystal packing but chain looseness in the amorphous region of DMF-treated PET fibers.

The average alignment and orientation of molecules along the fiber axis were determined by birefringence, which is listed in Table III. The birefringence of the DMF-treated PET fibers is smaller than that of untreated PET fiber. There is no proportional changes in birefringence with increasing DMF treatment temperature.

The decreases in birefringence suggests that decreases in the overall chain orientation along the fiber axis in the molecular structure of the sample fibers after DMF treatment has occurred. The chain disorientation can be explained by the irreversible dimension fiber changes with increasing treatment temperature.

The mechanism of shrinkage of the oriented semicrystalline PET fiber used in this study in DMF on heating and the changes in internal morphology

Table III Refractive Indices and Birefringence of DMF-Treated PET Fibers

Treatment	$n_{\parallel}$	$\perp$	Δn
Untreated	1.693	1.547	0.146
DMF-treated at			
100°C	1.694	1.551	0.143
120°C	1.694	1.552	0.142
140°C	1.696	1.553	0.143

of DMF-treated PET can be interpreted both in thermodynamic and in kinetic terms based on the observed experimental data and literature data suggested by other researchers[27,28] as follows: (1) the original stress in oriented noncrystalline regions would be removed by breaking down the internal molecular bonds between neighboring extended chains on heating above the glass transition temperature, and chain molecules would retract to be free or loosened; (2) crystallization of noncrystalline regions would occur after shrinkage. In the crystalline region, recrystallization of imperfect crystalline domains occurs by chain folding to stabilize the crystalline form. When existing small crystals melt,[24] shrunken chains may be recoiled.

In contrast to chain stretching, chain contraction shows decreases in the overall chain orientation through chain loosening, folding, and coiling during DMF treatment. However, a temperature effect is not found in the overall chain orientation, which suggests chain orientation in two different regions: crystalline orientation and amorphous orientation. However, we are not capable of knowing which region is affected in chain orientation by the birefringence method. Many researchers have shown that crystals in the crystalline region rearrange to become fewer, larger, and more perfect,[15,16] and remain oriented after DMF treatment, which gives rise to the possibility of disorientation in the noncrystalline region.

Tensile properties of DMF treated PET yarns were measured to examine the amorphous structure. The results are given in Table IV. Tenacity and yield stress of the fiber decreased as DMF treatment temperature increased. Even as DMF treatment improved crystallinity as shown in Table II, the fiber strength deteriorated. This suggests that tensile properties of PET fibers are influenced by the different aspects of fiber structure, such as the chain structure and chain orientation in the amorphous regions, which consists of fold surfaces, tie chains, and cilia chains in the end portions of molecules.

DMF treatment seems to break tie molecules, by which fibrils are held together, or intercrystalline links during DMF-induced recrystallization based on the fibril-lamella structure model, which is widely accepted. The strength of fibers is also affected by amorphous orientation. Avny, Rebenfeld, and Weigmann[11] obtained similar results and explained that tenacity is reduced due to chain disorientation in the amorphous region. This seems reasonable due to weakened interchain bonds in the disoriented structure according to the theory that chain slippage predominates in determining the strength of PET. In contrast, Patel and Bhat[30] reported that tenacity of DMF-treated PET is not changed and shows increases in some cases due to solvent-induced recrystallization.

DMF-treated PET shows increases in elongation with increasing treatment temperature. Shrinkage results in chain disorientation through chain folding, relaxation, loosening, and recoiling within the fibers as they are straightened and unfold, that makes fiber more extensible and less resistant to initial strain. Similar phenomena have been found in PETs treated with other solvents.[18]

Dyeing behavior of DMF-treated PET fibers with four disperse dyes, chosen due to their structural differences in size and shape, was studied to detect changes in void structure. Even as the total void content increases, the individual void size certainly becomes smaller after DMF treatment. Void-size distribution could be estimated from the dye uptake with various sizes of disperse dyes (Table V). In contrast to the large increases in dye uptake with p-nitroaniline, Solvent Yellow 3, and Disperse Red 15 after DMF treatment, there is no and little dye uptake with the bulkiest dye, Solvent Green 3, which means that void size is bigger than the dye volume of Disperse Red 15 (approximately 450 cubic Å) but smaller than that of Solvent Green 3 (approximately 4200 cubic Å). DMF treatment results in the greatest increase in the relative dye uptake of the larger dye Disperse Red 15. Lim et al.[14] have compared satu-

Table IV Tensile Properties of DMF-Treated PET Fibers

Treatment	Tenacity (g/tex)	Breaking Strain (%)	Initial Modulus	Yield Stress (g/tex)	Yield Strain (%)
Untreated	29.0	26.4	163.3	6.2	3.9
DMF-treated at					
100°C	27.2	38.4	104.5	5.1	5.2
120°C	26.4	45.6	89.7	4.7	5.7
140°C	22.4	54.9	62.8	4.3	6.6

Table V Dye Concentration and Relative Dye Uptake of DMF-Treated PET Fibers

Dye	*p*-Nitroaniline		Solvent Yellow 7		Disperse Red 15		Solvent Green 3	
Dyeing Time (h) Treatment	1/2	6	1/2	6	1/2	6	1/2	6
Untreated	111.1	148.5	169.2	203.8	23.4	70.9	0.505	3.841
DMF-treated at								
100°C	136.5	179.4	193.1	213.6	30.6	96.1	0.007	1.182
120°C	144.1	181.4	200.6	223.7	34.6	104.6	0.000	0.657
140°C	155.7	180.8	199.2	252.4	37.6	95.9	0.000	0.000

Dye concentration, μmol $\times 10^{-2}$/1 g of dry fabric.

ration dye uptake values using a series of anthraquinone dyes (which are smaller than Solvent green 3) and has suggested that larger or more bulky dyes are more accessible to the DMF-treated PET fiber. This would occur only when the voids are larger than the dyes in size. The voids should have sufficient space for the larger sized dye molecules to penetrate into the fiber, but the void size of DMF-pretreated fibers presumably is too small to permit diffusion of Solvent Green 3.

Densities of PET polymer have been used to account for void content in the amorphous region, as well as chain packing. This is measured in a nonpolar liquid medium of *n*-heptane and carbon tetrachloride, a relatively nonpenetrating medium that is capable of showing the presence of voids in a polymer; the less voids exist in polymer, the higher the density.[31] Contrasted to this earlier report, given DMF-treated fibers in this study show higher densities (Table II) with greater total void volume. This is explained by the fact that DMF-treated PET is much more crystalline than untreated PET, with only slightly increased void volume, therefore resulting in a net increase in crystallinity for the DMF-treated PET.

A decrease in initial modulus and yield stress in DMF-treated PET, which is given in Table IV, implies an increase of segmental mobility in the amorphous region. Weigmann and Ribnick[18] found that the initial modulus of the polyester yarns was the best property among mechanical properties to characterize the fiber–solvent system, and they estimated the interactions between the solvents and the PET yarn by the decrease in yarn elastic modulus, which were correlated with the solubility parameter (SP) of the solvents. SP of DMF (SP = 12.14) is very close to that of aliphatic ester residue (—O—CH_2—CH_2—O—OC—, SP = 12.1) in PET; therefore, DMF is quite able to disrupt the strong dipole interactions of carbonyl groups in PET, which leads to an increase in chain segmental mobility and results in a decrease in initial modulus of PET fiber. Also, an increase in segmental mobility might be attributed to a decrease in intermolecular bonding, a decrease in the taut tie molecule fraction, a chain disorientation, and an increase in chain folding, that leads to more extensibility and less resistant to initial strain. Therefore, the taut tie molecule fraction and segmental mobility in the amorphous region have been calculated on the basis of fiber Young's modulus. Moore and Weigmann[32] suggested that initial modulus was influenced by the structural parameters controlling dye diffusion rates. Yazdanian and Ward[26] showed that modulus is well correlated with *trans* content that governs amorphous orientation.

Diffusion coefficients (cm^2/s) of untreated and DMF-treated PET fibers were calculated using both the Crank and Hill equation. The results are given in Table VI. Diffusion rates of dye molecules into the DMF-treated PET fibers showed increases with all dyes except Solvent Green 3 with increasing DMF treatment temperature. The diffusion rate of Solvent Yellow 7 also decreases for PET treated with DMF at 140°C.

In many articles, segmental motion in the amorphous region has been found to be the major mechanism to account for dye diffusion rate into the PET fibers based on the free volume model, where diffusion coefficients are a function of the glass transition temperature. For the smaller dyes, the increases in diffusion rate in DMF-treated PET fibers confirm the increases in the segmental mobility in the fibers. This segmental mobility causes a continuous change in spatial arrangement of the polymer molecules in the amorphous region. Holes (voids) are created and disappear again. These free volumes provide sorption sites and diffusion channels through which the small dye molecules move from one site

to another. The increases in segmental mobility of the DMF-treated PET fibers could be attributed to more void formation and chain disorientation in the amorphous regions after DMF treatment.

Liquid diffusion behavior of the DMF-treated PET fibers was measured by CDT to characterize the intramolecular forces in the fiber. The results are shown in Table VII. Most CDTs decreased with increasing treatment temperature except for the CDT at 80°C in phenol with DMF-treated PET at 140°C.

Penetration of phenol into the amorphous regions involves the disruption of secondary forces and the production of segmental mobility of the polymer chains. Also, CDT has been used to detect the total void content in the polyester fiber because the PET molecules are too small to affect the diffusion rate, depending on the tortuosity and size of the voids. Several workers[15] have confirmed that solvent molecules easily diffuse into both the highly oriented and unoriented amorphous structure of polyester, while Lipp–Symonowicz[34] found no correlation between CDT and molecular orientation. In contrast, Weigmann et al.[19] showed that the CDT of DMF-treated polyester yarns increased with treatment temperature, which linearly correlated with density and crystallinity. It was suggested that formation or enlargement of crystallites leads to retardation of solubilization of the structure. In our study, DMF treatment of PET causes CDTs to decrease, while crystallinities and densities decrease. The different findings in the two studies are attributed to differences in the orientation of the two PETs used.

It has been reported that CDT of untreated PET is correlated with the nature of fibers,[35] mechanical properties,[36] density, dye absorption[37] (K/S values), crystallinity, crystallite size, molecular orientation (tortuosity of the diffusion channel), total void content, amorphous space, and stability of the crystalline portion.[15,33,38]

Table VII Critical Dissolution Time (CDT) of DMF-Treated PET Fibers

Treatment	CDT at 60°C (s)	CDT at 80°C (s)
Untreated	597	49.5
DMF-treated at		
100°C	470	21.2
120°C	281	16.4
140°C	274	24.5

In this study, it turned out that the diffusion behavior of solvent molecules in the DMF-treated PET fibers is very different compared with that of untreated PET, and that CDT of DMF-treated PET fiber is affected differently by the complex function of morphological structure parameters. Although solvent (phenol) diffusion behavior is not always correlated with dye diffusion behavior in PET fibers, it is similar to that of small dyes but not of the bulkiest dye. The controlling factors of diffusion for the two different diffusing molecules, phenol and disperse dye, must be different.

From the results, it is assumed that in the case of oriented and semicrystalline PET fiber after DMF treatment, CDT is promoted due to (1) the porous structure caused by increasing total void content, (2) a reduction of the tortuosity in the diffusion channels caused by decreases in taut tie molecules and molecular orientation, and (3) a decrease in intermolecular cohesive energy density caused by opening the structure.

Characterization of the Internal Morphology of the Graft Copolymers

The subsequent graft copolymerization of acrylic acid (AA) and methyl acrylate (MA) monomers onto DMF-pretreated PET fibers was carried out under optimal synthesis conditions and was expected to

Table VI Diffusion Coefficients ($\times 10^{-9}$ cm^2/s) of DMF-Treated PET Fibers

Dye	*p*-Nitroaniline		Solvent Yellow 7		Disperse Red 15		Solvent Green 3	
Equation	Crank	Hill	Crank	Hill	Crank	Hill	Crank	Hill
Treatment								
Untreated	6.20	15.82	7.63	21.94	1.21	2.24	0.19	0.32
DMF-treated at								
100°C	6.84	17.74	9.66	32.92	1.20	2.21	0.0004	0.001
120°C	7.88	21.39	10.05	33.50	1.37	2.54	0	0
140°C	10.18	31.13	8.55	23.01	2.11	4.06	0	0

Table VIII Physical Characteristics of Graft Copolymers

Treatment	Grafting (%)	Yarn Tex (g/km)	Fiber Diameter (μm)
Control,			
DMF-treated at			
100°C	—	35.9	13.17
120°C	—	37.7	13.54
140°C	—	40.0	14.19
DMF-treated, at	AA-grafted		
100°C,	12	39.6	14.06
120°C,	15	42.9	14.55
140°C,	19	44.2	15.13
DMF-treated, at	MA-grafted		
100°C,	20	41.2	14.33
120°C,	20	44.3	14.63
140°C,	20	47.2	14.88

give additional changes in the internal morphology of the fiber. Evidence of chemical changes in graft copolymers was detected by IR and DTA, even though these techniques do not provide conformation of covalent bond formation between the PET backbone and grafted branches. Scanning electron microscopy showed that the fiber surfaces of grafted PET contained no grafted polymer.

The physical characteristics of graft copolymers are listed in Table VIII. The properties of graft copolymers are compared with those of DMF-pretreated PET. Grafting results in weight gains and increases in fiber diameter and yarn tex due to introduction of copolymers into the DMF-treated PET. This changes the macrostructure and implies changes in the microstructure (internal morphology) of the graft copolymers.

Tensile properties of the graft copolymers were measured to understand how their chain structure affect orientation in the amorphous region of the fibers. Tensile properties of the grafted PET yarns with AA and MA are shown in Table IX. Overall grafting leads to a decrease in the mechanical properties: tenacity, initial modulus, and yield stress. Because the grafted copolymers have not been drawn to stretch the chains, the grafted branches of the noncrystalline polymers of PAA and PMA in the amorphous region of PET form partial phase segregated coils in the relaxed state. This results in loosening the PET chain structure causing chain disorientation in the amorphous PET regions. The chain disorientation leads to reduction of the van der Waal's forces between PET backbone chains, which makes it easier for chain stretch or chain slip-

Table IX Tensile Properties of the Control and Graft Copolymers

Treatment	Grafting (%)	Tenacity (g/tex)	Breaking Strain (%)	Initial Modulus	Yield Stress (g/tex)	Yield Strain (%)
Control,						
DMF-treated at						
100°C		27.2	38.4	104.5	5.1	5.2
120°C		26.4	45.6	89.7	4.7	5.7
140°C		22.4	54.9	62.8	4.3	6.6
DMF-treated, at	AA-grafted					
100°C,	12	23.0	32.9	89.7	5.3	5.3
120°C,	15	21.4	33.7	81.4	4.6	5.9
140°C,	19	19.0	36.7	51.1	4.0	7.2
DMF-treated, at	MA-grafted					
100°C,	20	23.4	31.6	80.4	5.2	6.1
120°C,	20	21.4	38.1	65.3	4.6	6.5
140°C,	20	18.7	43.3	47.3	4.4	8.7

page. The great number of hydrogen bonds that are expected between PAA in PET-*g*-PAA does not prevent chain slippage. It is assumed that PAA favors intramolecular hydrogen bonding due to the short distance between the chains, reducing the number of interchain hydrogen bonds. Moreover, grafting does not form intercrystalline links or tie molecules, and the branched chains in copolymers may cause the deformation of those already existing in PET. Similar results have been published, in which tenacity of PET-*g*-AA decreased with increasing graft yield.[39]

Breaking strain for the graft copolymers are intermediate between that of untreated polyester and DMF-treated polyester. This indicates that the graft copolymers in the amorphous regions reduced the effect of DMF treatment.

Refractive indices of the DMF-pretreated PET control fibers and graft copolymer samples were measured, and birefringences were calculated to determine the bulk chain orientation parallel to the fiber axis. The results are shown in Table X. Grafting results in a decrease in birefringence for both copolymers. This is probably caused by introduction of chain branches into the amorphous regions in PET. The branched PAA or PMA chains are expected to be atactic, and they are certainly disordered sequences or random arrangements that seem to interfere with the amorphous orientation, which causes a decrease in overall chain orientation in the copolymers.

In the case of PET homopolymer, chain orientation has been interpreted to cause resistance for dyes or liquids diffusing in the radial direction of the fiber; however, in the case of graft copolymers, it does not affect these properties such as maximum dye uptake, CDT, and T_g, as will be discussed later. Therefore, the chain orientation of graft copolymer does not correlate with its sorption-diffusion phenomenon and segmental mobility.

It is widely known that only the amorphous region is attacked by reagents during the grafting. Because grafted PAA and PMA chains are atactic and cannot crystallize, introduction of additional amorphous PAA or PMA polymer chains into the PET fiber matrix would not be expected to reduce or affect the original crystalline portion in PET, but would alter the ratio between the crystalline and amorphous region to give a decrease in the crystallinity due to an increase in the amorphous weight in graft copolymers. Based on above information, the degree of crystallinity of graft copolymers was calculated. The results are shown in Table XI. This "apparent crystallinity" of graft copolymer fibers shows decreases with increasing graft yields, as expected.

Table X Refractive Indices and Birefringence of Control and Graft Copolymers

Treatment	Grafting (%)	$n_{\parallel}$	$n_{\perp}$	Δn
Control, DMF-treated at				
100°C		1.694	1.551	0.143
120°C		1.694	1.552	0.142
140°C		1.696	1.553	0.143
DMF-treated, at	AA-grafted			
100°C,	12	1.679	1.549	0.130
120°C,	15	1.675	1.549	0.126
140°C,	19	1.674	1.550	0.124
DMF-treated, at	MA-grafted			
100°C,	20	1.670	1.546	0.124
120°C,	20	1.669	1.545	0.124
140°C,	20	1.665	1.545	0.120

The density of graft copolymer fibers was measured and calculated. The calculated density values of PET-*g*-PAA fibers showed a continuous increase with graft uptake. This can be accounted for by the addition of the higher density (ρ = 1.585 g/cm^3) grafted PAA. However, the measured densities of PET-*g*-PAA fibers increased slightly as graft uptake increased, and they were much lower than calculated density values. This might be due to a decrease in molecular packing of the polymer. Grafted branches are expected to lead to two results: chain compactness by filling in between the control PET backbones, and chain loosening by pulling the control PET chains farther apart. The branched PAA may pull the PET backbones more than block them.

In contrast to the results of PET-*g*-PAA, the measured densities of PET-*g*-PMA copolymers decreased dramatically with increasing graft uptake. This can be interpreted by the introduction of the lower density (ρ = 1.220 g/cm^3) grafted PMA compared to that of original PET. The measured density values are higher than calculated density values. This might be due to an increase in chain packing of the fibers. The increases in the observed fiber diameter imply changes in the open structure of the fiber, where the branched PMA chain block the space in the control chains more than pull the PET backbone chains apart.

Unexpectedly, in this study, molecular packing of the copolymers did not correlate with the void content in amorphous region of the fiber. PET grafted with PAA results in lower molecular packing

Table XI Crystallinity of Control and Graft Copolymers

Treatment	Grafting (%)	Crystallinity by Density (%)	Crystallinity by Calculation (%)
Control,			
DMF-treated at			
100°C		48.1	—
120°C		50.1	—
140°C		51.7	—
DMF-treated, at	AA-grafted		
100°C,	12	—	42.3
120°C,	15	—	42.7
140°C,	19	—	43.0
DMF-treated, at	MA-grafted		
100°C,	20	—	38.5
120°C,	20	—	40.1
140°C,	20	—	41.4

with less void content, while PET grafted with PMA establishes higher molecular packing with greater void content. This shows the same trend as DMF-treated PET with more chain compactness and void volume.

Disperse dyeing properties of the copolymers were examined and explained in the view of void structure and segmental mobility in the amorphous region. The grafted samples were compared with the DMF-pretreated samples. Dye uptake of graft copolymer samples for short and extended dyeing times were measured to determine the total void volume and to correlate dye uptake with other properties. Dye concentrations on the graft copolymers are listed in Table XII.

AA grafting lowered the dyeability of PET with p-Nitroaniline, Solvent Yellow 7, and Disperse Red 15. The dye uptakes with these dyes of all AA-grafted samples decreased with increasing graft uptake, whereas the dyeability of AA-grafted PET fibers with Solvent Green 3 was promoted. Still, maximum dye uptake of the fibers decreased with increasing graft uptake. MA grafting enhanced the dye uptake for all four disperse dyes used. Solvent Yellow 7 is shown to have the highest and Solvent Green 3 the lowest dye affinity.

In PET fibers, dye uptake is not always correlated with the amorphous area but with total void content in amorphous regions that is the total volume of the accessible sites for dyes. Therefore, total void content can be determined from the maximum dye adsorption of the smaller-sized disperse dye molecules of which dye diffusion is not governed by void shape and tortuosity, whereas diffusion is not governed by void shape and tortuosity, whereas diffusion of larger-sized dyes is affected by void tortuosity due to molecular size and orientation.[33]

As the above theory for PET is applied to the graft copolymers, MA grafting results in an increase, while AA grafting leads to a decrease in the total void volume. Introduction of both AA and MA grafts could cause blockage of some of the original voids by "filling them in," but the grafts also might create new voids between PET chains by pulling PET chains farther apart. This might explain the observed increases in fiber diameter. In the case of AA grafting, the strong secondary forces present due to the many inter- and intrachain hydrogen bonds could limit the formation of new voids within the grafted branches. Maximum dye uptake in the copolymer is well correlated with its CDT and T_g, but not its birefringence.

Void size was compared with the size of four disperse dye molecules which vary from 226 to 4200 cubic Å. Specific dye structure was sensitive to changes in the amorphous structure. The bulkiest dye Solvent Green 3 was markedly different than other dyes in maximum dye adsorption.

Both AA and MA grafting result in an increase in individual void size presumably due to loosening the PET chains and creation of new and larger voids. Those voids are large enough for Solvent Green 3 to diffuse into and to be held in the fiber.

The rod-like dye Solvent Yellow 7 showed the highest dye-fiber affinity in both AA- and MA-grafted fibers. Dyeing of Solvent Yellow 7 into voids with its rod-like shape might be more favorable due to the higher substantivity between the dye and the

Table XII Dye Concentration of Control and Graft Copolymers

Dye Dyeing time (h) Treatment	Grafting (%)	*p*-Nitroaniline		Solvent Yellow 7		Disperse Red 15		Solvent Green 3	
		1/2	6	1/2	6	1/2	6	1/2	6
Control, DMF-treated at									
100°C		136.5	179.4	193.1	213.6	30.6	96.1	0.007	1.182
120°C		144.1	181.4	200.6	223.7	34.6	104.6	0.000	0.657
140°C		155.7	180.8	199.2	252.4	37.6	95.9	0.000	0.000
DMF-treated, at	AA-grafted								
100°C,	12	122.7	156.5	166.5	201.3	51.1	92.3	1.574	9.563
120°C,	15	108.6	144.4	150.2	198.2	45.8	89.9	2.192	8.345
140°C,	19	105.7	135.4	147.9	180.2	43.2	84.5	2.725	7.123
DMF-treated, at	MA-grafted								
100°C,	20	140.6	187.1	230.9	361.2	46.6	89.2	5.679	11.00
120°C,	20	144.2	191.8	218.1	333.2	45.4	91.8	8.395	12.34
140°C,	20	166.6	224.3	219.9	438.0	44.3	101.0	9.282	20.03

Dye concentration, μmol $\times 10^{-2}$/1 g of dry fabric

polymer chains. As shown in Table XIII, diffusion coefficients of PET-*g*-PAA fibers with the smaller dyes are greater than those of PET-*g*-PMA fibers, but lower with the larger dyes that are sensitive to the segmental mobility in the graft copolymers. The cause of blocking of diffusion of Solvent Green 3 in PET treated with DMF at higher temperatures is unknown.

Solvent diffusion behavior in the copolymer fibers was examined to determine internal molecular forces present by critical dissolution time (CDT). The results are shown in Table XIV. Liquid diffusion of phenol into all samples and CDT at the higher temperature (80°C) is markedly accelerated compared to the lower temperature (60°C).

Pure phenol, being smaller than dye molecules, can diffuse into the fiber structure much more easily because it requires a much lower activation energy. Also, the shape and tortuosity of the voids will have a negligible effect on the rate of diffusion. In the first stage of CDT measurement, phenol does not break the covalent bonds, but it causes disruptions between chains and breaks down the intermolecular forces, such as van der Waals forces and hydrogen

Table XIII Diffusion Coefficients ($\times 10^{-9}$ cm^2/s) of Control and Graft Copolymers

Dye Equation Treatment	Grafting (%)	*p*-Nitroaniline		Solvent Yellow 7		Disperse Red 15		Solvent Green 3	
		Crank	Hill	Crank	Hill	Crank	Hill	Crank	Hill
Control, DMF-treated at									
100°C		6.84	17.74	9.66	32.92	1.20	2.21	0.0004	0.001
120°C		7.88	21.39	10.05	33.50	1.37	2.54	0	0
140°C		10.18	31.13	8.55	23.01	2.11	4.06	0	0
DMF-treated, at	AA-grafted								
100°C,	12	8.28	22.13	9.22	26.33	4.13	8.81	0.36	0.63
120°C,	15	8.15	20.92	8.28	21.39	3.74	7.74	1.00	1.79
140°C,	19	9.51	25.28	10.51	29.71	4.08	8.43	2.29	4.37
DMF-treated, at	MA-grafted								
100°C,	20	7.90	20.24	5.72	13.06	3.82	7.96	3.73	7.74
120°C,	20	8.24	21.13	6.25	14.47	3.57	7.29	6.75	16.00
140°C,	20	8.32	21.11	3.80	7.82	2.90	5.74	3.24	6.30

Table XIV Critical Dissolution Time (CDT) of Control and Graft Copolymers

Treatment	Grafting (%)	CDT at 60°C (s)	CDT at 80°C (s)
Control, DMF-treated at			
100°C		470	21.2
120°C		281	16.4
140°C		274	24.5
DMF-treated, at	AA-grafted		
100°C,	12	597	81.5
120°C,	15	549	80.6
140°C,	19	689	93.4
DMF-treated, at	MA-grafted		
100°C,	20	364	2.7
120°C,	20	115	2.7
140°C,	20	263	3.8

bonds, completely. Therefore, CDT determines cohesive energy density, which is a measure of the amount of energy required to overcome all intermolecular forces in 1 mol of liquid.

The temperature effect might be due to increased segmental agitation, which begins around PET's T_g. In the case of PET-*g*-PMA, all bonds interacting between molecular chains apparently are broken, because 80°C is high enough above the glass transition temperature for the PET-*g*-PMA. The incorporation of soft and rubbery PMA in the rigid PET structure promotes segmental mobility, which is well correlated with reduced cohesive energy density, thereby increasing the ability of the solvent to diffuse into the copolymer PET-*g*-PMA. Contrary to PMA, the PAA in PET restricts mobility due to the higher molecular cohesive energy caused by the higher polarity of the PAA fiber. This leads to a decrease in solvent diffusion into the copolymer PET-*g*-PAA.

In this study, the different chemical compositions of the graft copolymers influence solvent diffusion behavior. CDT is well correlated with segmental mobility (from T_g) and the total void volume (from the results of dye uptake), but it is not governed by chain orientation (from birefringence) or the total volume of the amorphous regions. However, the increases in CDT of PET-*g*-PMA pretreated with DMF at 140°C is not explained by the observed results.

Another important role of solvent dissolution is classification of the mode of polymer structure between linear (or branched) and crosslinked polymers. Solvent can pull apart and dissolve linear and branched polymers by replacing the interchain secondary bonds in PET and copolymer chains. However, these polymer–solvent secondary bonds cannot overcome primary valence crosslinks, so crosslinked polymers are not soluble but swell extensively. Therefore, it was proved that the copolymers synthesized were branched polymers, namely graft copolymers.

The glass transition temperatures (T_g) of the graft copolymer samples were measured to obtain the information about their chain segmental mobility, which begins around the T_g above which polymers become soft and plastic. The results are shown in Table XV. As a result, there is a single T_g for each graft copolymer and it is shifted to lower or higher temperatures due to the presence of the copolymer. The T_gs of homopolymer PET, PMA, and PAA are known to be 69°C, 5°C,[40] and 105°C,[41] respectively. The graft copolymers have intermediate T_g values between those of the two homopolymers.

The results show that the T_gs of the graft copolymers are affected by the two monomers differently. The rubbery PMA branches have little effect on steric hindrance to rotation, and they force the main chains farther apart, destroying the multiple van der Waals forces accounting for main chain interactions between PET molecules, increasing the free volume, which could result in the more flexible chain molecules in PET. Kellman et al.[43] found the same trend with the graft copolymer of poly(styrene-*g*-methyl acrylate).

However, in the case of PAA grafting, stronger secondary forces (hydrogen bonds) must form as a firm network between PAA branches and hold to-

Table XV Glass Transition Temperature (T_g) of Control and Graft Copolymers

Treatment	Grafting (%)	T_g (°C)
Control, DMF-treated at		
100°C		70.7
120°C		71.5
140°C		73.0
DMF-treated, at	AA-grafted	
100°C,	12	105.0
120°C,	15	102.5
140°C,	19	101.0
DMF-treated, at	MA-grafted	
100°C,	20	65.5
120°C,	20	66.0
140°C,	20	64.8

gether the amorphous region. This higher intrinsic cohesive density could lead to the restriction of segmental movement. The hydrogen bonds will be destroyed at a higher temperature, which would make for a higher T_g for PET-*g*-PAA copolymer. In addition, the decreased free volume of PET-*g*-PAA, found in dyeing studies suggest a raise in the T_g. In contrast to this result, Kim et al.[44] obtained the lowered T_gs for PET backbone polymer as AA grafting increases, which was explained by the branching effect.

CONCLUSIONS

The photo-induced graft copolymerization of AA and MA monomers onto DMF-pretreated PET fiber was carried out using liquid and vapor phase photografting techniques. Graft uptake was dependent on DMF pretreatment, DMF pretreatment temperature, amount of DMF retention in the fiber, and synthesis conditions.

DMF-pretreatment of PET before graft copolymerization causes the changes in the internal morphology of fiber that results in increases in total void content and degree of crystallinity, but causes decreases in amorphous chain orientation and individual void size. These factors enhance the diffusion properties of the monomers into the PET fiber and promote the grafting effect.

The graft copolymerization of PET with flexible and uncrystallizable PMA forces the main chains and branched chains farther apart and disrupts secondary forces between the chains, which results in increases in the total void content, individual void size and chain segmental mobility, and decreases in chain orientation and degree of crystallinity.

The graft copolymerization of PET with brittle and ionic PAA results in increases in polarity and cohesive-energy density and individual void size and decreases in total void content, segmental mobility, chain orientation, and degree of crystallinity.

REFERENCES

1. I. R. Bellobono and E. Selli, in *Photopolymerisation and Photoimaging Science and Technology,* N. S. Allen, Ed., Elsevier Applied Science, New York, 1989, p. 115.
2. H. Kubota, K. Kobayashi, and Y. Ogiwara, *Polym. Photochem.,* **7,** 379 (1986).
3. H. Kubota and Y. Ogiwara, *J. Appl. Polym. Sci.,* **38,** 717 (1989).
4. H. L. Needles and K. W. Alger, *J. Appl. Polym. Sci.,* **22,** 3405 (1978).
5. Y. Ogiwara, H. Kuboda, and T. Yasunaga, *J. Appl. Polym. Sci.,* **19,** 887 (1975).
6. Y. Okiwara, K. Torikoshi, and H. Kuboda, *J. Polym. Sci., Polym. Lett. Ed.,* **20,** 17 (1982).
7. R. P. Seiber and H. L. Needles, *J. Appl. Polym. Sci.,* **19,** 2187 (1975).
8. S. A. Siddiqui, K. McGee, W.-C. Lu, K. Alger, and H. L. Needles, *Am. Dyestuff Rep.,* **70,** 20 (1981).
9. S. Tazuke, T. Matoba, H. Kimura, and T. Okada, *Modification of Polymers,* ACS Symposium Series 121, American Chemical Society, Washington, DC, 1980, p. 217.
10. Z. P. Yao and B. Rånby, *J. Appl. Polym. Sci.,* **41,** 1459 (1990).
11. Y. Avny, L. Rebenfeld, and H.-D. Weigmann, *J. Appl. Polym. Sci.,* **22,** 125 (1978).
12. Y. Ogiwara, M. Kanda, M. Takumi, and H. Kuboda, *J. Polym. Sci., Polym. Lett. Ed.,* **19,** 457 (1981).
13. S. Kuwabara, *Sen-i Gakkaishi,* **34**(9), 56 (1978).
14. Y.-J. Lim, M. Tahara, T. Takagishi, N. Kuroki, and T. Wakida, *Sen-i Gakkaishi,* **40**(6), 88 (1984).
15. H. L. Needles and C. Walker, *J. Appl. Polym. Sci., Appl. Polym. Symp.,* **47,** 249 (1991).
16. T. Takagishi, T. Wakida, and N. Kuroki, *Sen-i Gakkaishi,* **34**(12), 48 (1978).
17. T. Wadanabe, M. Miyoshi, T. Takahashi, and I. Tsujimoto, *Sen-i Gakkaishi,* **33**(5), 35 (1977).
18. H.-D. Weigmann and A. S. Ribnick, *Textile Res. J.,* **44,** 165 (1974).
19. H.-D. Weigmann, M. G. Scott, A. S. Ribnick, and L. Rebenfeld, *Textile Res. J.,* **46,** 574 (1976).
20. H.-D. Weigmann, M. G. Scott, A. S. Ribnick, and R. D. Matkowsky, *Textile Res. J.,* **47,** 745 (1977).
21. A. Cunningham and I. M. Ward, *Polymer,* **15,**, 749 (1974).
22. L. D'Esposito and J. L. Koenig, *J. Polym. Sci., Polym. Phys. Ed.,* **14,** 1731 (1976).
23. A. S. Ribnick, H.-D. Weigmann, and L. Rebenfeld, *Textile Res. J.,* **42,** 720 (1972).
24. J. T. Guthrie, M. Ryder, and F. I. Abdel-Hay, *Polym. Bull.,* **1,** 501 (1979)
25. K. K. Mocherla and J. P. Bell, *J. Polym. Sci., Polym. Phys. Ed.,* **11,** 1779 (1973).
26. M. Yazdanian and I. M. Ward, *Polymer,* **26,** 1779 (1985).
27. W. E. Morton and J. W. S. Hearle, *Physical Properties of Textile Fibers,* The Textile Institute and Butterworth & Co., London, 1975.
28. A. S. Ribnick, *Textile Res. J.,* **39,** 742 (1969)
29. A. S. Ribnick and H.-D. Weigmann, *Textile Res. J.,* **43,** 316 (1973).
30. V. H. Patel and N. V. Bhat, *Indian J. Textile Res.,* **11,** 181 (1986)

31. E. L. Lawton and D. M. Cates, *J. Appl. Polym. Sci.*, **13,** 899 (1969).
32. R. A. F. Moore and H.-D. Weigmann, *Textile Chem. Colorist,* **15,** 197 (1983).
33. A. K. Kulshreshtha, M. V. S. Rao, and N. E. Dweltz, *J. Appl. Polym. Sci.*, **30,** 3423 (1985).
34. B. Lipp–Symonowicz, in *Morphology of Polymers,* Walter de Gruyter & Co., Berlin, 1986, p. 610.
35. V. Rossbach and D.-I. N. Karunaratna, *Melliand Textilberichte* (Eng. Ed.), **66,** 260 (1985).
36. R. S. Chauhan and N. E. Dweltz, *Textile Res. J.*, **55,** 385 (1985).
37. F. Galil, *Textile Res. J.*, **43,** 615 (1973).
38. M. L. Gulrajani and R. K. Saxena, *Textile Res. J.*, **50,** 406 (1980).
39. J.-S. Shim and H.-I. Kim, *Polymer,* **6,** 406 (1982).
40. L. J. M. Francisca and A. V. R. Reddy, *Eur. Polym. J.*, **27**(7), 627 (1991).
41. *Encyclopedia of Polymer Science and Engineering,* John Wiley & Son, New York, 1985. p. 226, p. 260.
42. H. L. Needles, S. Holmes, and M.-J. Park, *J. Soc. Dyers Colorists,* **106,** 385 (1990).
43. R. Kellman, D. T. J. Hill, D. S. Hunter, and J. H. O'Donnell, in *Radiation Effects on Polymers,* R. L. Clough and S. W. Shalaby, Eds., ACS Symposium Series 475, American Chemical Society, Washington, DC, 1991, p. 199.
44. H. D. Kim, D. L. Kim, and T. I. Chun, *J. Korean Soc. Text. Eng. Chemists,* **21,** 32 (1984).

Received February 23, 1995
Accepted September 15, 1995